

## Supporting Information

### Self-Assembly of Monolayer Vesicles via Backbone-Shiftable Synthesis of Janus Core-Shell Bottlebrush Polymer

Jiyun Nam,<sup>†</sup> YongJoo Kim,<sup>‡</sup> Jeung Gon Kim,<sup>§</sup> and Myungeun Seo<sup>\*,†,‡,||</sup>

<sup>†</sup>Graduate School of Nanoscience and Technology, Korea Advanced Institute of Science and  
Technology (KAIST), Daejeon 34141, Republic of Korea

<sup>‡</sup>KAIST Institute for the Nanocentury, KAIST, Daejeon 34141, Republic of Korea

<sup>§</sup>Department of Chemistry and Research Institute of Physics and Chemistry, Jeonbuk  
National University, 567 Baekje-daero, Deokjin-gu, Jeonju-si, Jeollabuk-do 54896, Republic  
of Korea

<sup>||</sup> Department of Chemistry, KAIST, Daejeon 34141, Republic of Korea

\*To whom should be addressed: [seomyungeun@kaist.ac.kr](mailto:seomyungeun@kaist.ac.kr) (M.S.)

#### **This supplementary information includes:**

Materials and Methods

Supporting Scheme 1

Supporting Figures S1 – S21

Supporting Tables S1 – S2

Supporting References

## Materials and Methods

**Materials.** Unless otherwise noted, all the chemicals were used as received. Grubbs 3<sup>rd</sup> generation catalyst was kindly provided by Materia, Inc (Pasadena, CA). 1,8-Diazabicyclo[5,4,0]undec-7-ene (DBU, 98%) were purchased from Sigma-Aldrich (St. Louis, MO) and stored in a glovebox. *N*-(3-Dimethylaminopropyl)-*N'*-(ethylcarbodiimide hydrochloride (EDC) were purchased from Tokyo Chemical Industry (Tokyo, Japan). 4-Dimethylaminopyridine (DMAP) ( $\geq 99\%$ ), *cis*-5-norbornene-*exo*-2,3-dicarboxylic anhydride ( $\geq 99\%$ ), *exo*-3,6-epoxy-1,2,3,6-tetrahydrophthalic anhydride ( $\geq 99\%$ ), 6-aminohexanoic acid (99%), ethanolamine ( $\geq 99\%$ ), triethylamine ( $\geq 99\%$ ) and ethyl vinyl ether ( $\geq 99\%$ ) were purchased from Sigma-Aldrich. *N*-(Carboxylhexanoyl)-*cis*-5-norbornene-*exo*-2,3-dicarboximide was synthesized following literature procedure.<sup>1</sup> 1-(2-Hydroxyethyl)-1H-pyrrole-2,5-dione was prepared following literature procedure.<sup>2</sup> Aluminium oxide (basic, Brockmann I) were purchased from Acros (Waltham, MA). Styrene (99%) and n-butyl acrylate (nBA) (99%) were purchased from Sigma-Aldrich and filtered over basic alumina prior to use. The chain transfer agent, 2-hydroxyethyl 2-(((dodecylthio)carbonothioyl)-thio)-2-methylpropanoate) (CTA) was afforded by esterification of (S)-1-dodecyl-(S')-( $\alpha,\alpha'$ -dimethyl- $\alpha''$ -acetic acid) trithiocarbonate with ethylene glycol in excess following the procedure published elsewhere.<sup>3</sup> Using the CTA as an initiator, polylactide macro-chain transfer agent (PLA-CTA) was prepared following literature procedure.<sup>4</sup> Both d-lactide (99%) and l-lactide (99%) were kindly provided by Corbion Purac (Amsterdam, Netherlands). d,l-Lactide was obtained from recrystallizing the same amount of d-lactide and l-lactide in ethyl acetate.

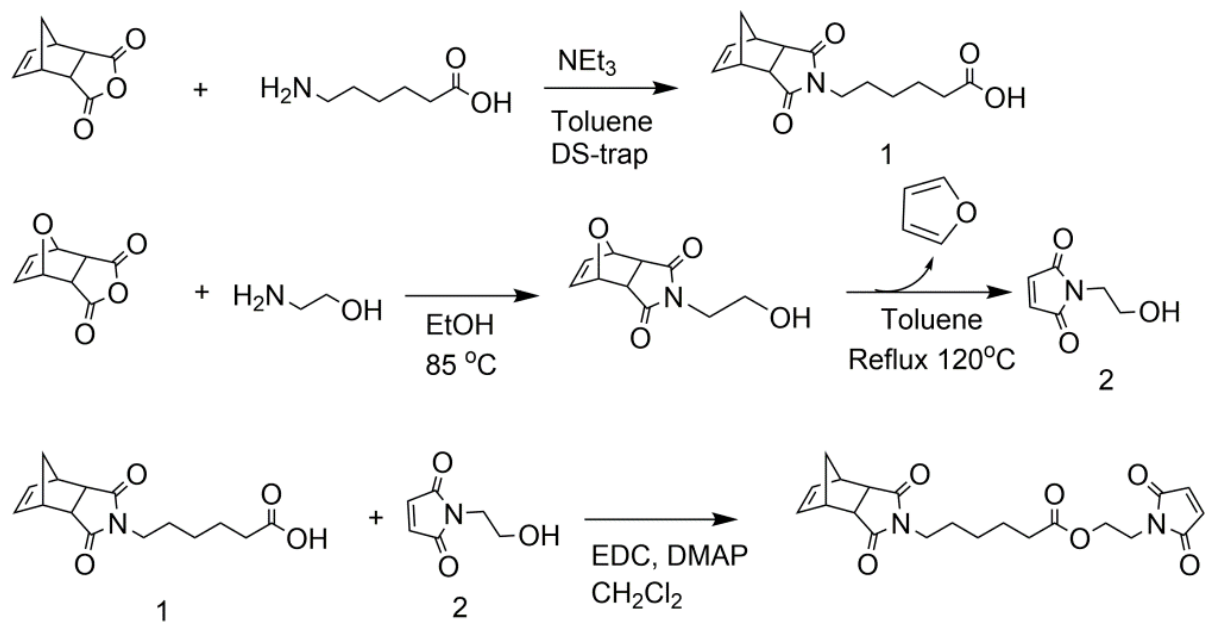
Benzoic acid (99.5%) and other laboratory chemicals used in work-up process were purchased from Daejung (Siheung, Korea). Azobisisobutyronitrile (AIBN) and methanol ( $\geq 99.8\%$ ) were purchased from Junsei (Tokyo, Japan) or Sigma-Aldrich. AIBN was recrystallized from methanol and stored at  $-20\text{ }^{\circ}\text{C}$ . All the HPLC grade solvents were purified using a solvent purification system (C&T International, Suwon, Korea). HPLC grade toluene, tetrahydrofuran (THF) and dichloromethane (DCM) were purchased from Burdick & Jackson (Morristown, NJ), Daejung (Siheung, Korea), and J. T. Baker (Center Valley, PA), respectively.

**Methods.**  $^1\text{H}$  nuclear magnetic resonance (NMR) spectroscopy was conducted on a Bruker Avance 400 MHz spectrometer (Billerica, MA) in  $\text{CDCl}_3$  using the residual NMR solvent signal as an internal reference at 7.26 ppm. The molar mass and dispersity ( $D$ ) of polymer were measured using an Agilent Infinity 1260 series (Santa Clara, CA) size exclusion chromatography (SEC) system equipped with an Optilab T-rEX refractive index detector (Santa Barbara, CA) and PLgel 10  $\mu\text{m}$  MIXED-B columns. Chloroform was used as an eluent at  $35\text{ }^{\circ}\text{C}$ , and the number-average molar masses ( $M_{n,\text{SEC}}$ ) of the polymers were calculated relative to linear polystyrene standards (EasiCal) purchased from Agilent Technologies. Weight-average absolute molecular masses ( $M_{w,\text{MALLS}}$ ) were determined by using a Wyatt DAWN8+ multi-angle laser light scattering (MALLS) detector (Santa Barbara, CA) equipped to SEC.  $dn/dc$  values were obtained for each injection by assuming 100% mass elution from the columns. Mass spectra were obtained on a Bruker Daltonik microTOF-QII mass spectrometer using the electrospray ionization method. Elemental analysis was conducted using a Thermo Scientific FLASH 2000 series elemental analyzer (Waltham, MA). Dynamic light scattering (DLS) measurements were performed on a Brookhaven 90Plus/BI-MAS particle size analyzer (Holtsville, NY) at wavelength of 658 nm with scattering angle of  $90^{\circ}$ .

Samples were prepared at a concentration of 2 mg mL<sup>-1</sup> and filtered through 0.2 µm PTFE syringe filters prior to the measurements. Transmission electron microscopy (TEM) was performed on a FEI Talos F200X (Hillsboro, OR, USA) field-emission transmission electron microscope with acceleration voltage of 200 kV. Samples were prepared on 300 mesh carbon-coated copper grids by dropping the solution (10 mg mL<sup>-1</sup>) and evaporation of the solvent. The samples were stained by exposing RuO<sub>4</sub> vapor prior to imaging. Scanning transmission electron microscopy (STEM) images and energy dispersive X-ray spectroscopy (EDX) maps were also collected on a FEI Talos F200X microscope operated at 200 kV.

**Synthesis of *N*-(1H-Pyrrole-2,5-dione-1H-ethylhexanoate)-*cis*-5-norbornene-*exo*-2,3-dicarboxiimide (NFM).** NFM bearing a maleimide group responsible for the SUMI reaction was synthesized following the route shown in Scheme S1, and characterized by <sup>1</sup>H, <sup>1</sup>H-<sup>1</sup>H and <sup>13</sup>C NMR spectra as shown in Figures S1 – S2. In a round-bottomed flask (RBF) equipped with a stir bar, 1-(2-hydroxyethyl)-1H-pyrrole-2,5-dione (**2**)<sup>2</sup> (2 g, 14.16 mmol) were placed under inert atmosphere. EDC (2.76 g, 14.38 mmol) and DMAP (0.12 g, 0.97 mmol) were added to the RBF followed by DCM (10 mL) under N<sub>2</sub> atmosphere. *N*-(carboxylhexanoyl)-*cis*-5-norbornene-*exo*-2,3-dicarboxiimide (**1**)<sup>1</sup> (0.41 g, 1.49 mmol) was dissolved in DCM (5 mL) and added to the flask via syringe. The reaction mixture was allowed to stir under argon at room temperature overnight. After washing with water (20 mL), drying over MgSO<sub>4</sub>, and concentrating in a rotary evaporator, the crude product was purified by silica gel chromatography with ethyl acetate/hexane = (3/7 v/v) as an eluent to give 1.5 g of NFM as a white powder (75 % yield). <sup>1</sup>H NMR (400 MHz, CDCl<sub>3</sub>): δ 6.74 (s, 2H), 6.28 (s, 2H), 4.22 (t, J = 4 Hz, 2H), 3.78 (t, J = 8 Hz, 2H), 3.45 (t, J = 8 Hz, 2H), 3.27 (s, 2H), 2.67 (s, 2H), 2.26 (t, J = 8 Hz, 2H), 1.50 – 1.64 (m, 6H), 1.35 – 1.25 (m, 2H); <sup>13</sup>C NMR (101 MHz, CDCl<sub>3</sub>): δ 24.4, 28.8, 27.8, 33.9, 37.1, 38.7, 43.0, 45.4, 49.0, 61.5, 134.5, 139.0, 170.7, 173.4, 179.3; ESIMS

m/z: calcd: 423.1634; found: 423.1566 [M + H]<sup>+</sup>; elemental analysis calcd (%) for C<sub>21</sub>H<sub>24</sub>N<sub>2</sub>O<sub>6</sub>:  
C 62.98, H 6.09, N 6.86, O 23.59.



**Scheme S1.** Synthesis of NFM

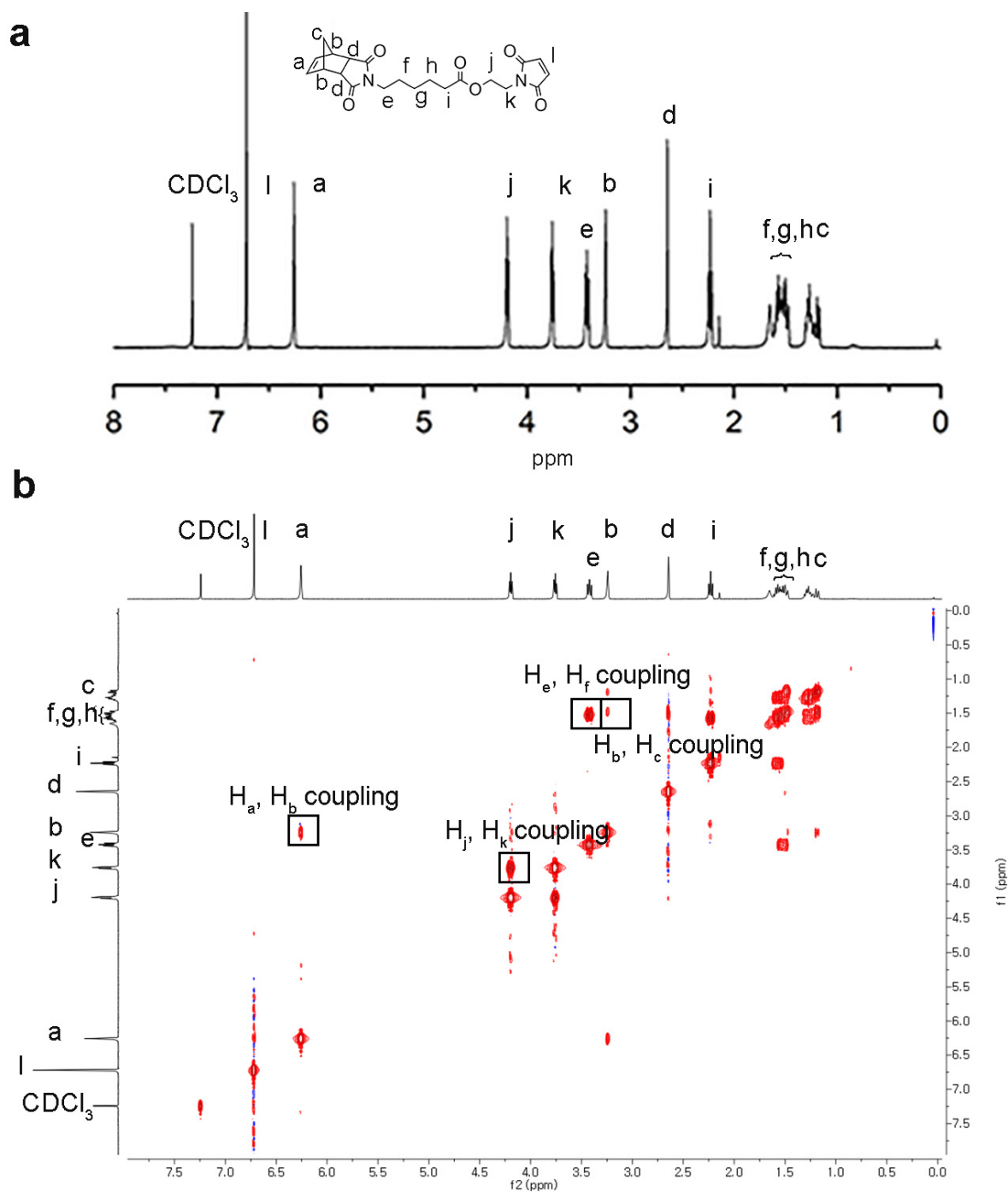


**Figure S1.** (a)  $^1\text{H}$  NMR and (b)  $^1\text{H}$ - $^1\text{H}$  COSY NMR spectrum of NFM (400 MHz,  $\text{CDCl}_3$ ).

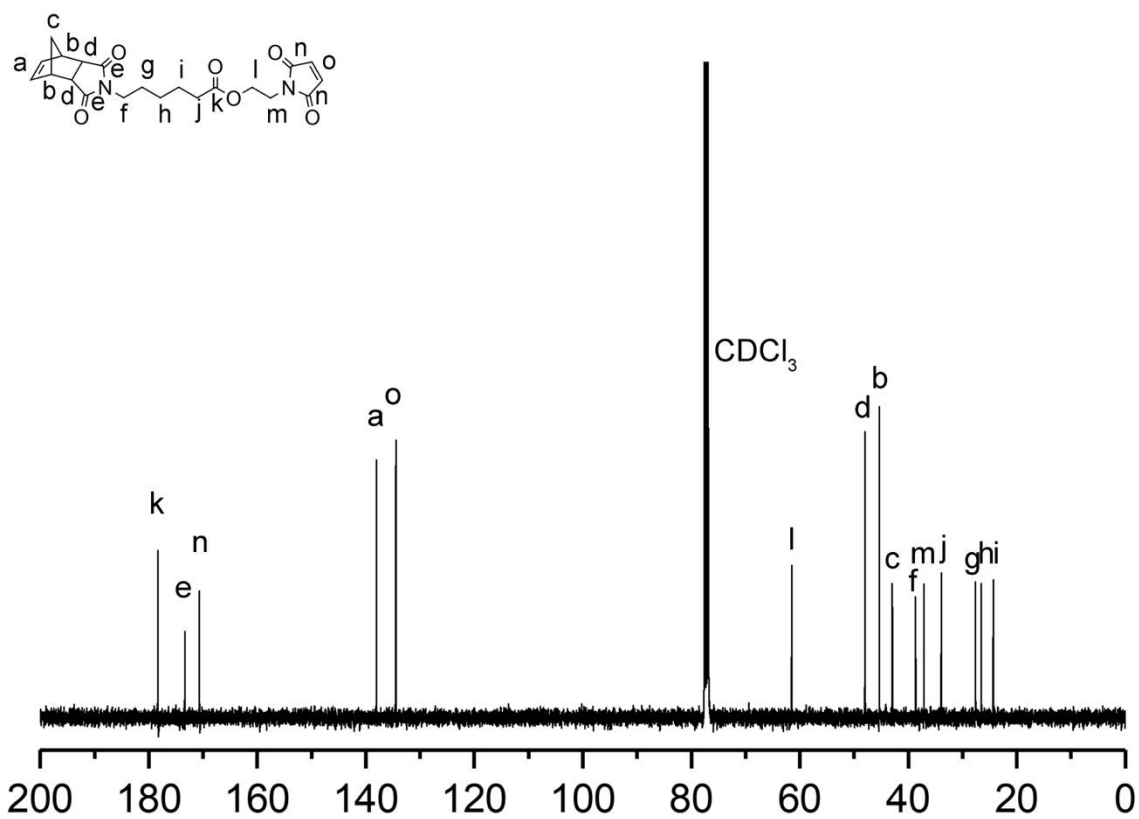


**Figure S2.** <sup>13</sup>C NMR spectrum of NFM (100 MHz, CDCl<sub>3</sub>).

**RAFT polymerization protocol.** A polymerization mixture containing CTA, a monomer, AIBN as a radical initiator, and toluene as a solvent was prepared according to the composition summarized in Table S1, and transferred into a Schlenk flask. The reaction mixture was degassed by three freeze-pump-thaw cycles and then heated to a designated temperature (60 or 120 °C). After a certain times lapse, the polymerization was quenched by cooling the reaction to room temperature and exposed to air. We did not pursue high conversion so the polymer could be obtained in a reasonable time with minimized termination. The polymer product was collected by precipitation in methanol and filtration, and then dried under vacuum for overnight.

**Table S1.** Synthetic details of RAFT polymerizations employed in this study

Product	CTA	Monomer ([M]:CTA)	Initiator (eq) <sup>a</sup>	Solvent (v/v) <sup>b</sup>	Temp. (°C)	Polymerization time (h)	Conv. (%) <sup>c</sup>
PS <sub>19</sub>	CTA	50 : 1	none	none	120	6	47
PS <sub>19</sub> - <i>branch</i> -PS <sub>38</sub>	PS <sub>19</sub> - <i>branch</i>	100 : 1	none	none	120	2	31
PS <sub>19</sub> - <i>branch</i> -PS <sub>55</sub>	PS <sub>19</sub> - <i>branch</i>	100 : 1	none	none	120	3	52
PLA <sub>28</sub> - <i>b</i> - PS <sub>21</sub>	PLA <sub>28</sub> -CTA	100 : 1	none	none	120	2.5	23
PLA <sub>28</sub> - <i>b</i> - PS <sub>21</sub> - <i>branch</i> -PS <sub>19</sub>	PLA <sub>28</sub> - <i>b</i> - PS <sub>21</sub> - <i>branch</i>	50 : 1	none	toluene (3)	120	6	44
PLA <sub>28</sub> - <i>b</i> - PS <sub>21</sub> - <i>branch</i> -	PLA <sub>28</sub> - <i>b</i> - PS <sub>21</sub> - <i>branch</i> -PS <sub>19</sub>	20 : 1	0.1	toluene (7)	60	24	42

PS <sub>19</sub> - <i>b</i> - PnBA <sub>10</sub>							
PLA <sub>31</sub> - <i>b</i> - PS <sub>40</sub>	PLA <sub>31</sub> -CTA	100 : 1	none	none	120	3	47
PLA <sub>31</sub> - <i>b</i> - PS <sub>40</sub> - <i>branch</i> -PS <sub>15</sub>	PLA <sub>31</sub> - <i>b</i> - PS <sub>40</sub> - <i>branch</i>	50 : 1	none	toluen e (3)	120	8	28
PLA <sub>31</sub> - <i>b</i> - PS <sub>40</sub> - <i>branch</i> - PS <sub>15</sub> - <i>b</i> - PnBA <sub>13</sub>	PLA <sub>31</sub> - <i>b</i> - PS <sub>40</sub> - <i>branch</i> - PS <sub>15</sub>	20 : 1	0.1	toluen e (7)	60	24	53

<sup>a</sup>Equivalent to CTA

<sup>b</sup>Volume of the solvent relative to the monomer volume

<sup>c</sup>Determined by <sup>1</sup>H NMR analysis

**SUMI reaction.** A solution of a macro-CTA (1.0 equiv), NFM (2.0 equiv) and AIBN (0.1 equiv) in THF (ca. 3 mL) was prepared in a 10-mL glass ampoule, and degassed by three freeze-pump-thaw cycles. The ampoules were sealed under vacuum and heated to 60 °C. After 6 h, the reaction mixture was cooled to room temperature, exposed to air, and then precipitated into methanol. The polymer was collected by filtration and dried under vacuum for overnight.

**DP and  $M_{n,NMR}$  calculation.** DP and  $M_{n,NMR}$  of PS-*branch*-PS' BMMs and PLA-*b*-PS-*branch*-PS-*b*-PnBA BMMs were determined by integration of the <sup>1</sup>H NMR spectra. In case of BMMs, integration of the peaks at 7.24 – 6.31 ppm corresponding to the H<sub>d</sub> aromatic protons of PS repeating units was calculated with respect to two H<sub>a</sub> protons (3.33 – 3.18 ppm) originating from the CTA as a reference (Figure S3). The aromatic proton integral value was used to determine the degree of polymerization (DP) and  $M_{n,NMR}$  of PS. Then the aromatic proton peak was used as a reference for integration of other peaks in <sup>1</sup>H NMR spectra of PS-*branch* (Figure S4), particularly the end group peaks at 4.25 – 3.25 ppm, so the SUMI efficiency could be

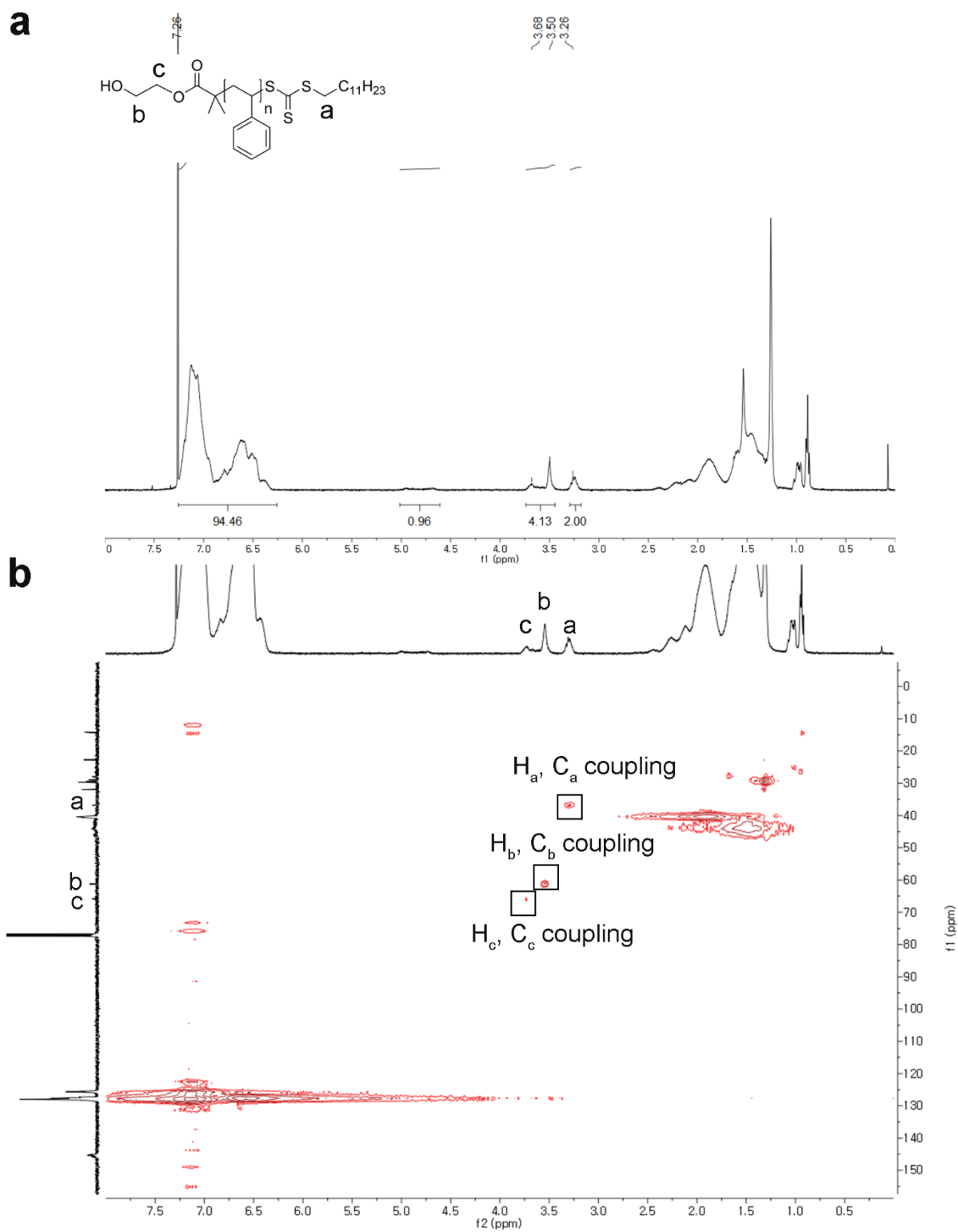
determined. This collective integral value was kept the same for integration of PS-*branch*-PS's (Figures S5 - S6), and DP of the PS' block was determined from the increase in the aromatic proton integral.

In case of BMMMs, DP and  $M_{n,NMR}$  of PLA was calculated by comparing the integral values of the peak corresponding to the H<sub>a</sub> methine proton of PLA repeating units (5.33 – 5.01 ppm) to the two H<sub>d</sub> protons (3.29 – 3.16 ppm) originating from the CTA as a reference (Figure S7 and S12). By taking the methine proton peak of PLA repeating units as a reference, integration of the peaks corresponding to the H<sub>e</sub> aromatic protons of PS repeating units (7.24 – 6.31 ppm) and that corresponding to the signals of the H<sub>m</sub> methylene protons adjacent to the ester in PnBA repeating units (4.19 – 3.72 ppm) gave DP and  $M_{n,NMR}$  of PS, PS', and PnBA, respectively (Figures S8 – S11 and Figures S13 – S16).

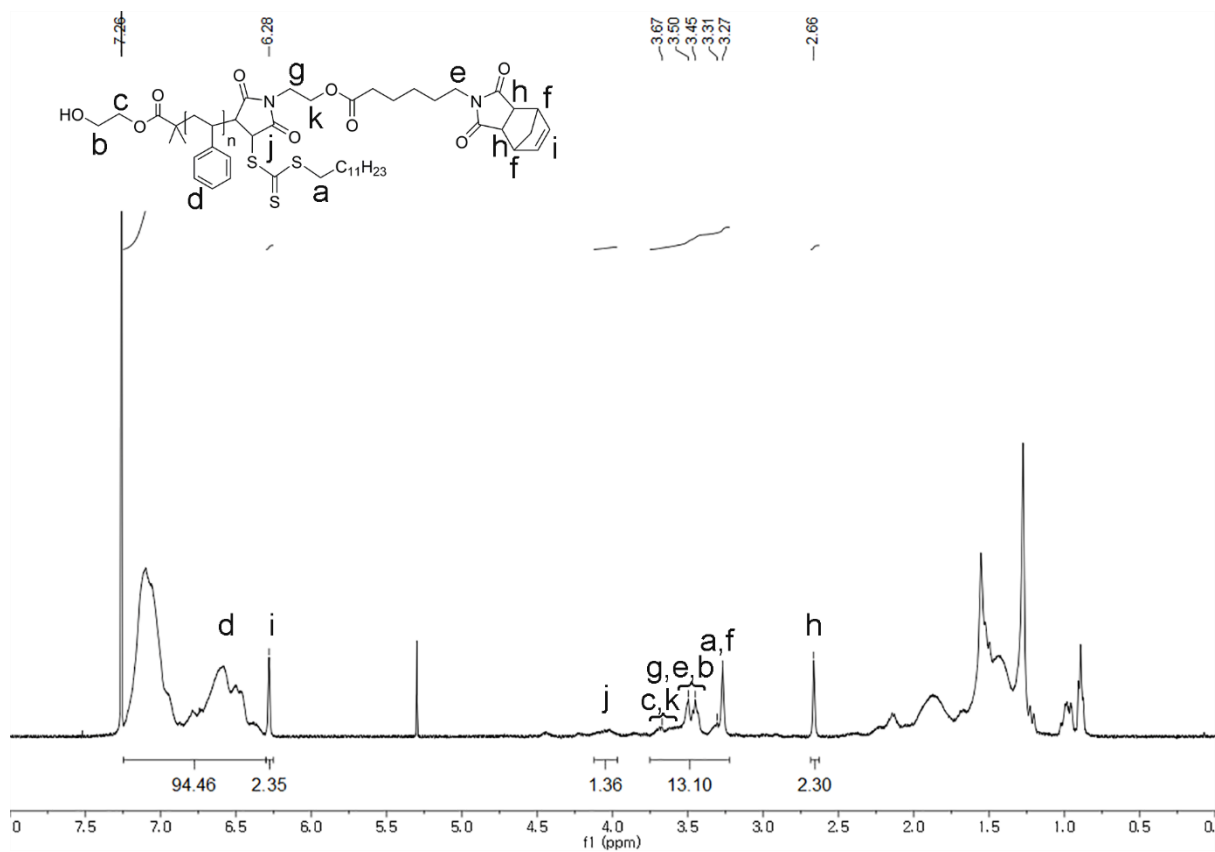
**ROMP protocol.** A macromonomer was placed in an oven-dried, 2-mL reaction vial equipped with a stir bar and dissolved in a solvent in a glovebox. A stock solution of Grubbs 3<sup>rd</sup> generation catalyst was prepared separately, and injected into the macromonomer solution to initiate the polymerization at room temperature. After a certain time lapse, the reaction mixture was quenched with several drops of ethyl vinyl ether. The reaction mixture was then concentrated and precipitated into methanol. The polymeric product was recovered by filtration and dried under vacuum for overnight. Table S2 summarizes detailed information for the syntheses of DGBCPs.

**Table S2.** Synthetic details of ROMP reactions employed in this study

Entry	MM	[MM] 0:[Ru] 0	Solvent	[MM] 0 (M)	Time (h)
DGBCP(30)-PS <sub>19</sub> /PS <sub>38</sub>	PS <sub>19</sub> - <i>branch</i> -PS <sub>38</sub>	30 : 1	THF	0.03	1
DGBCP(50)-PS <sub>19</sub> /PS <sub>38</sub>	PS <sub>19</sub> - <i>branch</i> -PS <sub>38</sub>	50 : 1	THF	0.025	1.2
DGBCP(30)-PS <sub>19</sub> /PS <sub>55</sub>	PS <sub>19</sub> - <i>branch</i> -PS <sub>55</sub>	30 : 1	THF	0.015	1
DGBCP(50)-PS <sub>19</sub> /PS <sub>55</sub>	PS <sub>19</sub> - <i>branch</i> -PS <sub>55</sub>	50 : 1	THF	0.01	2
DGBCP(30)-[PLA <sub>28</sub> - <i>b</i> -PS <sub>21</sub> ]/ [PS <sub>19</sub> - <i>b</i> -PnBA <sub>10</sub> ]	PLA <sub>28</sub> - <i>b</i> -PS <sub>21</sub> - <i>branch</i> -PS <sub>19</sub> - <i>b</i> - PnBA <sub>10</sub>	30 : 1	toluene	0.03	2
DGBCP(50)-PLA <sub>28</sub> - <i>b</i> -PS <sub>21</sub> ]/ [PS <sub>19</sub> - <i>b</i> -PnBA <sub>10</sub> ]	PLA <sub>28</sub> - <i>b</i> -PS <sub>21</sub> - <i>branch</i> -PS <sub>19</sub> - <i>b</i> - PnBA <sub>10</sub>	50 : 1	toluene	0.01	2
DGBCP(30)-[PLA <sub>31</sub> - <i>b</i> -PS <sub>40</sub> ]/ [PS <sub>15</sub> - <i>b</i> -PnBA <sub>13</sub> ]	PLA <sub>31</sub> - <i>b</i> -PS <sub>40</sub> - <i>branch</i> -PS <sub>15</sub> - <i>b</i> - PnBA <sub>13</sub>	30 : 1	toluene	0.025	2
DGBCP(50)-[PLA <sub>31</sub> - <i>b</i> -PS <sub>40</sub> ]/ [PS <sub>15</sub> - <i>b</i> -PnBA <sub>13</sub> ]	PLA <sub>31</sub> - <i>b</i> -PS <sub>40</sub> - <i>branch</i> -PS <sub>15</sub> - <i>b</i> - PnBA <sub>13</sub>	50 : 1	toluene	0.015	2



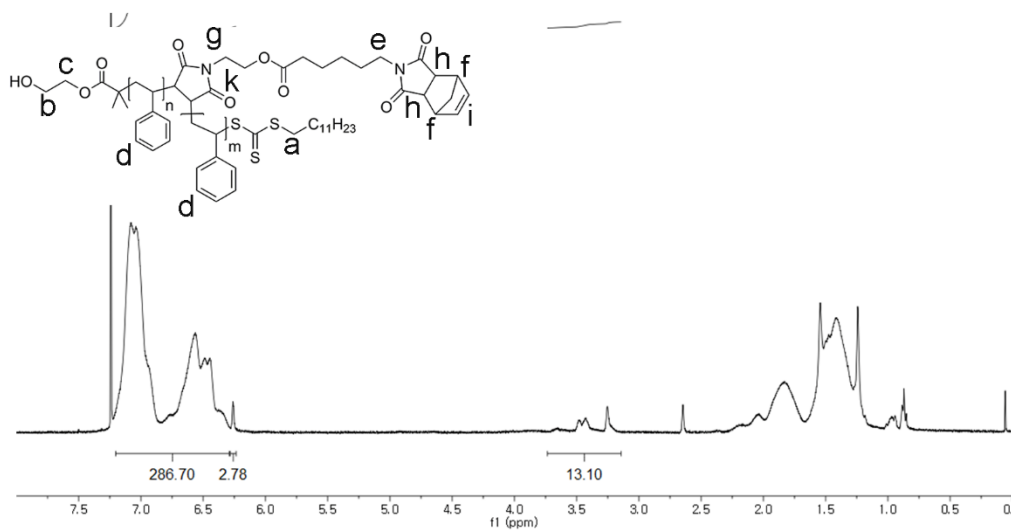
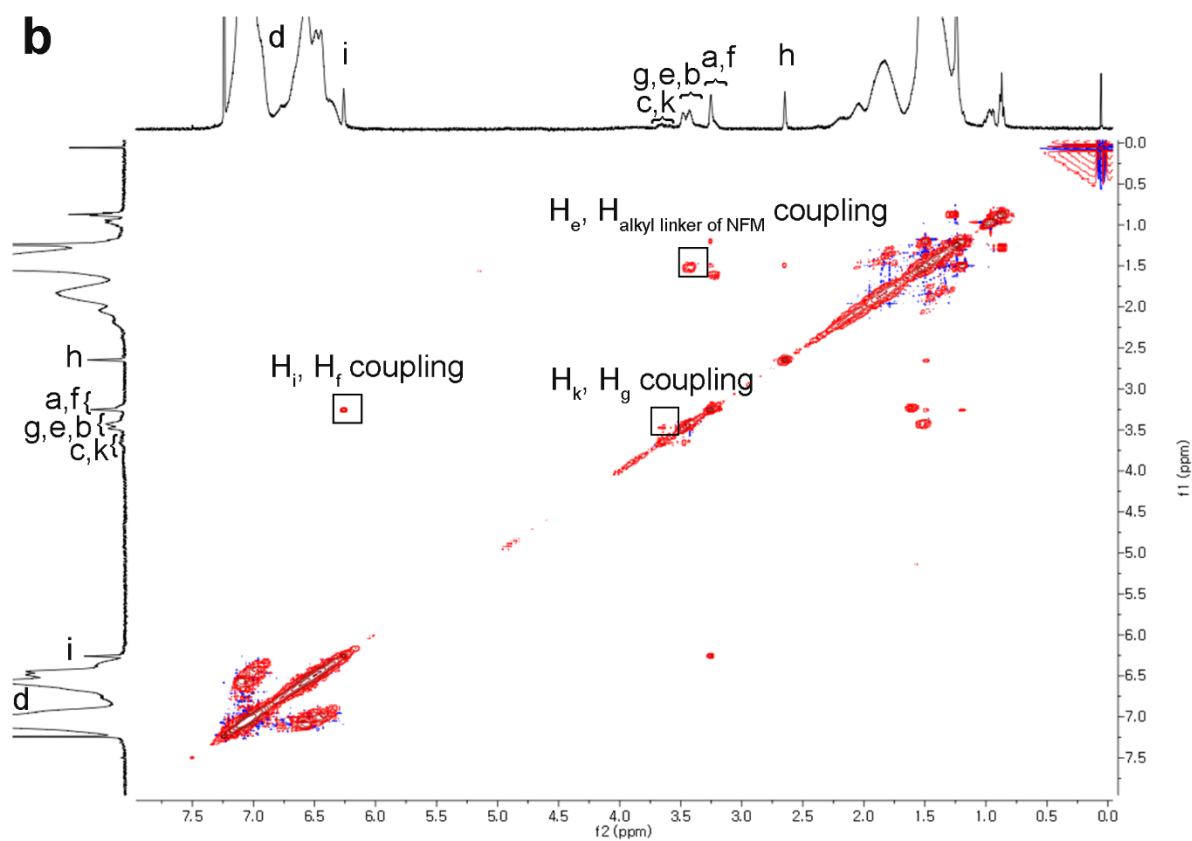
**Figure S3.** (a) <sup>1</sup>H NMR and (b) <sup>1</sup>H-<sup>13</sup>C HSQC NMR spectrum of PS<sub>19</sub> (400 MHz, CDCl<sub>3</sub>).



**Figure S4.** <sup>1</sup>H NMR spectrum of PS<sub>19</sub>-branch (400 MHz, CDCl<sub>3</sub>).

**a**

$$\text{SUMI efficiency} = \frac{\text{Experimental proton resonance signal of NFM (f,g,e,c,k) and CTA (a,b)}}{\text{Theoretical proton resonance signal of NFM (f,g,e,c,k) and CTA (a,b)}} = \frac{13.10}{14.00} = 94\%$$

**b**

**Figure S5.** (a)  $^1\text{H}$  NMR and (b)  $^1\text{H}$ - $^1\text{H}$  COSY NMR spectrum of PS<sub>19</sub>-branch-PS<sub>38</sub> (400 MHz, CDCl<sub>3</sub>).

**a**

$$\text{SUMI efficiency} = \frac{\text{Experimental proton resonance signal of NFM (f,g,e,c,k) and CTA (a,b)}}{\text{Theoretical proton resonance signal of NFM (f,g,e,c,k) and CTA (a,b)}} = \frac{13.10}{14.00} = 94\%$$

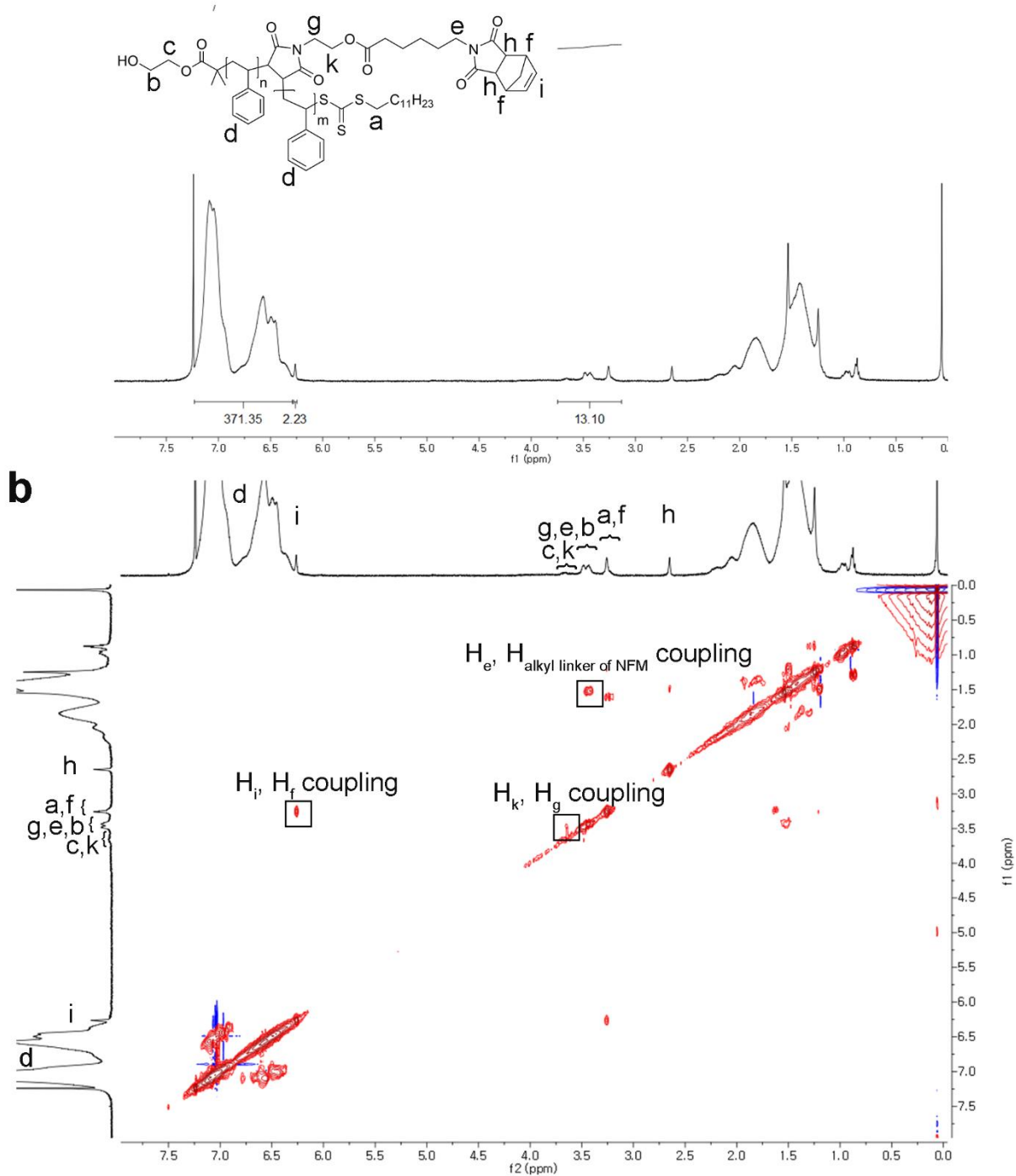


**Figure S6.** (a) <sup>1</sup>H NMR and (b) <sup>1</sup>H-<sup>1</sup>H COSY NMR spectrum of PS<sub>19</sub>-branch-PS<sub>55</sub> (400 MHz, CDCl<sub>3</sub>).

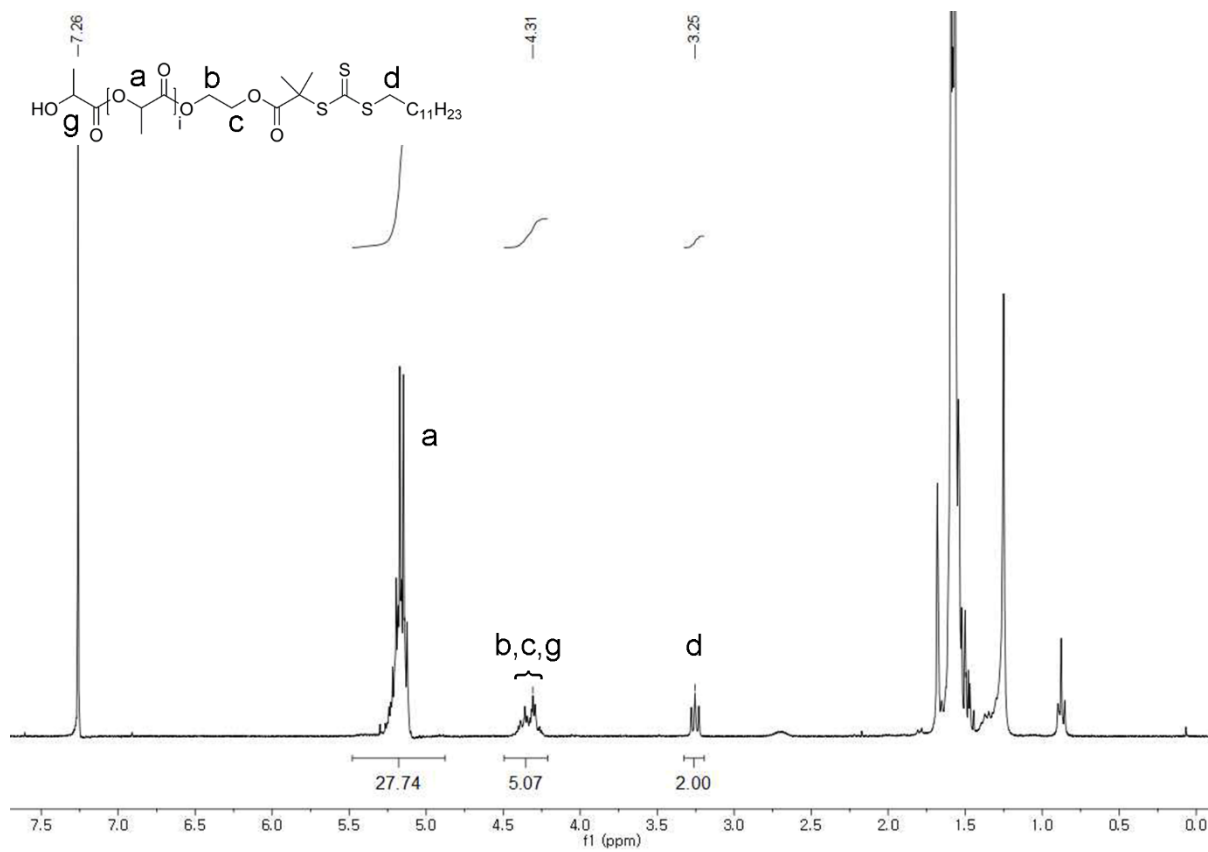


**Figure S7.** <sup>1</sup>H NMR spectrum of PLA<sub>28</sub> (400 MHz, CDCl<sub>3</sub>).

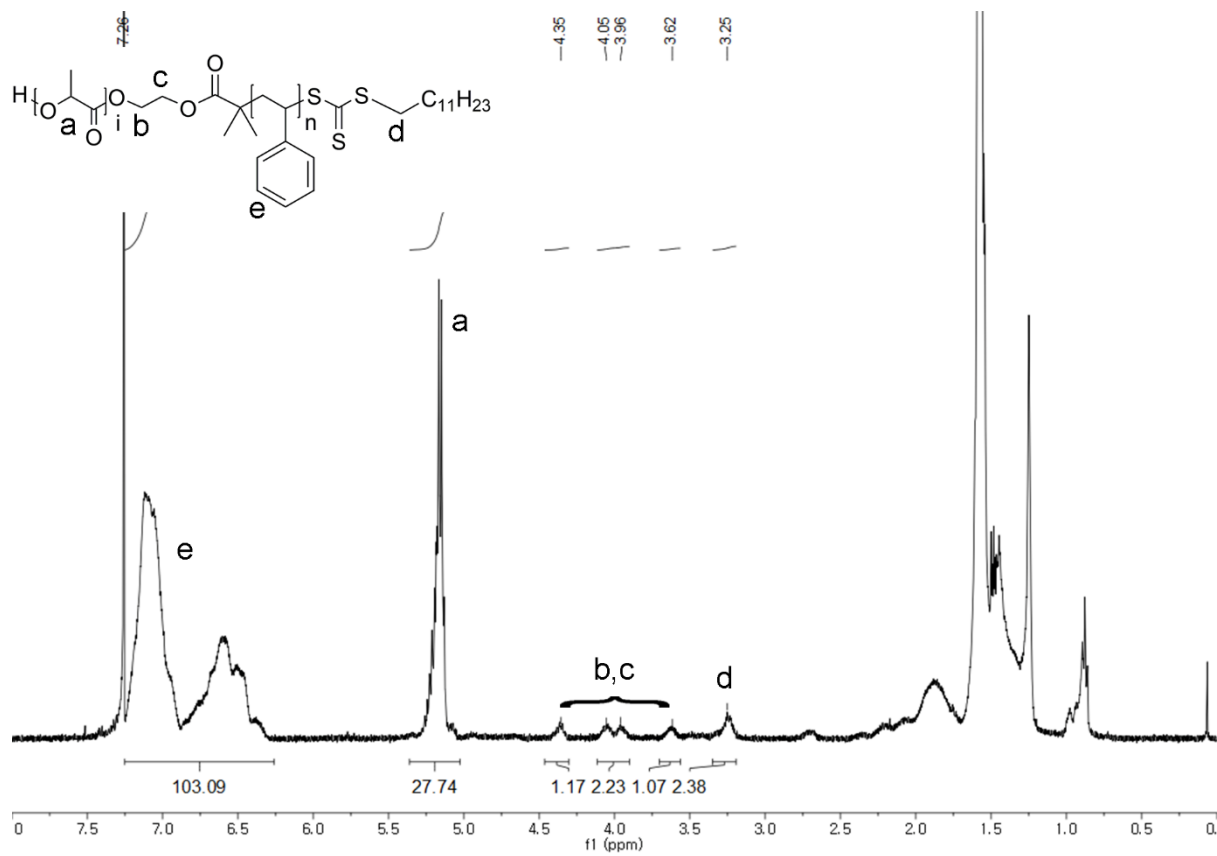


**Figure S8.** <sup>1</sup>H NMR spectrum of PLA<sub>28</sub>-b-PS<sub>21</sub> (400 MHz, CDCl<sub>3</sub>).

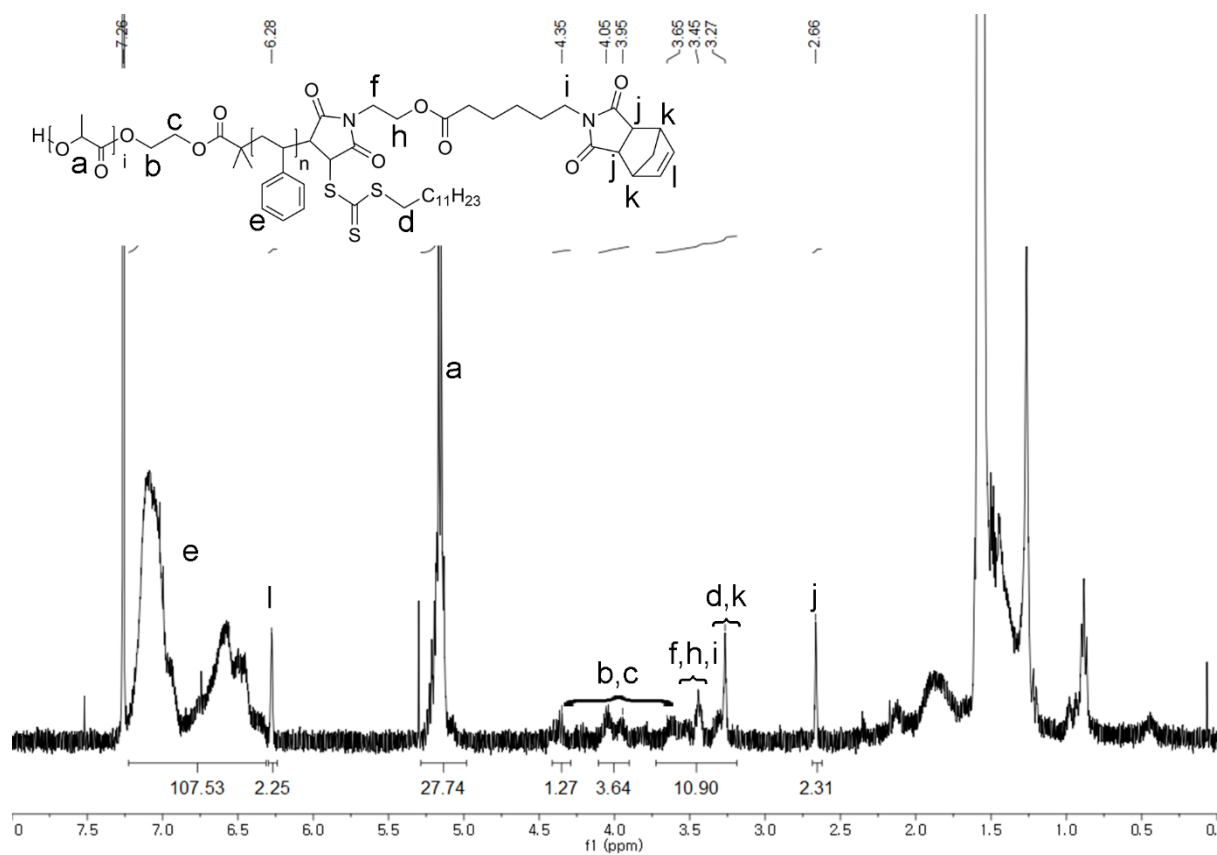


**Figure S9.** <sup>1</sup>H NMR spectrum of PLA<sub>28</sub>-b-PS<sub>21</sub>-branch (400 MHz, CDCl<sub>3</sub>).

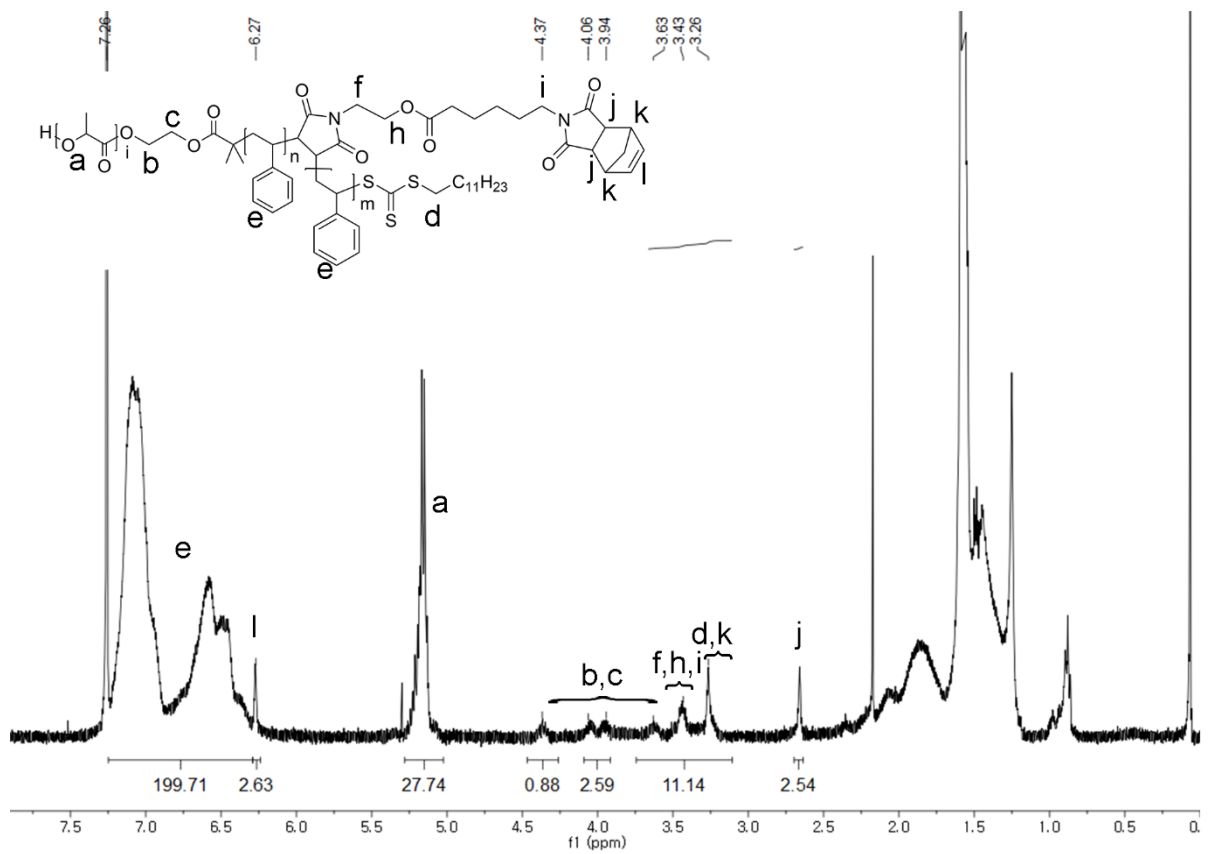


**Figure S10.** <sup>1</sup>H NMR spectrum of PLA<sub>28</sub>-b-PS<sub>21</sub>-branch-PS<sub>19</sub> (400 MHz, CDCl<sub>3</sub>).

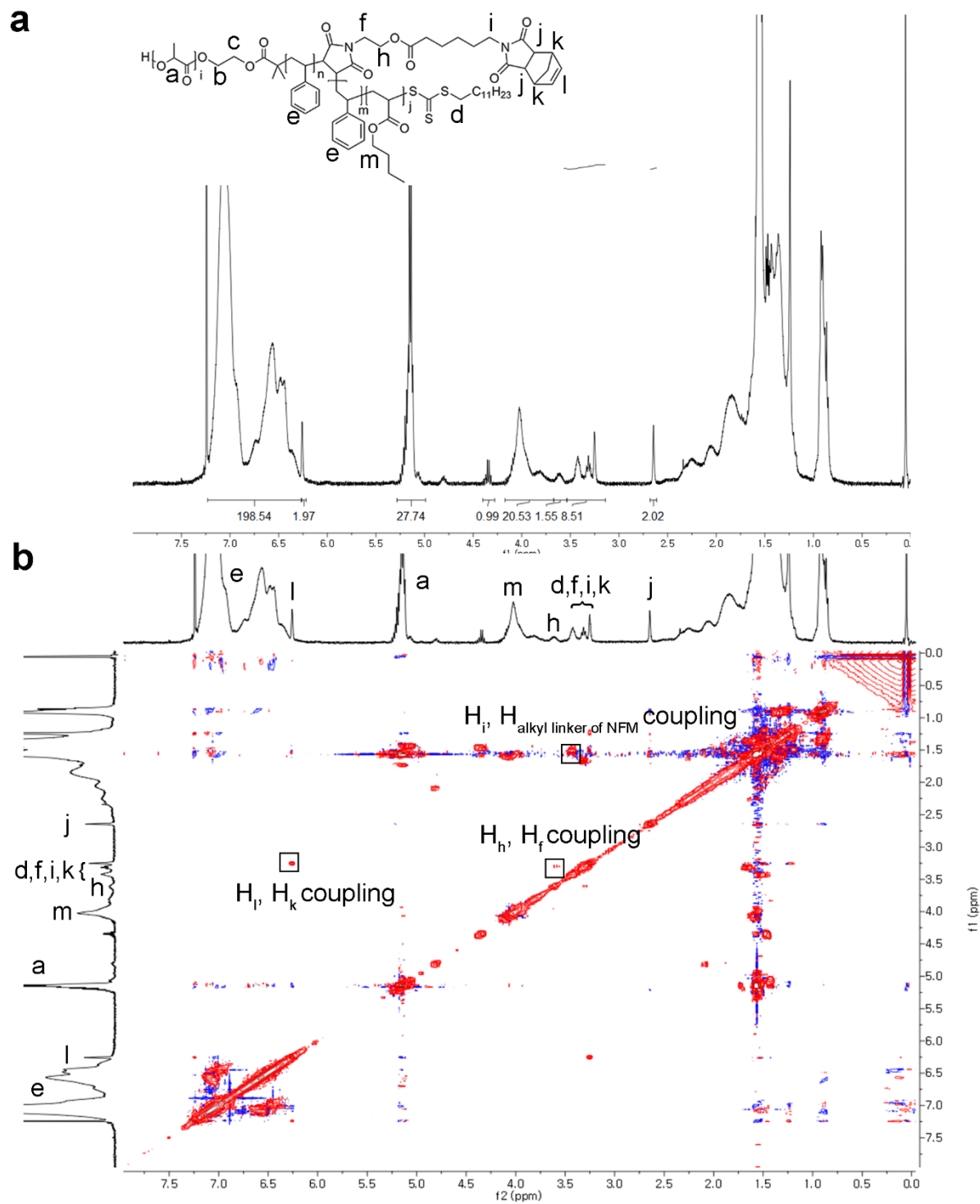


**Figure S11.** (a) <sup>1</sup>H NMR and (b) <sup>1</sup>H-<sup>1</sup>H COSY NMR spectrum of PLA<sub>28</sub>-*b*-PS<sub>21</sub>-branch-PS<sub>19</sub>-*b*-PnBA<sub>10</sub> (400 MHz, CDCl<sub>3</sub>).

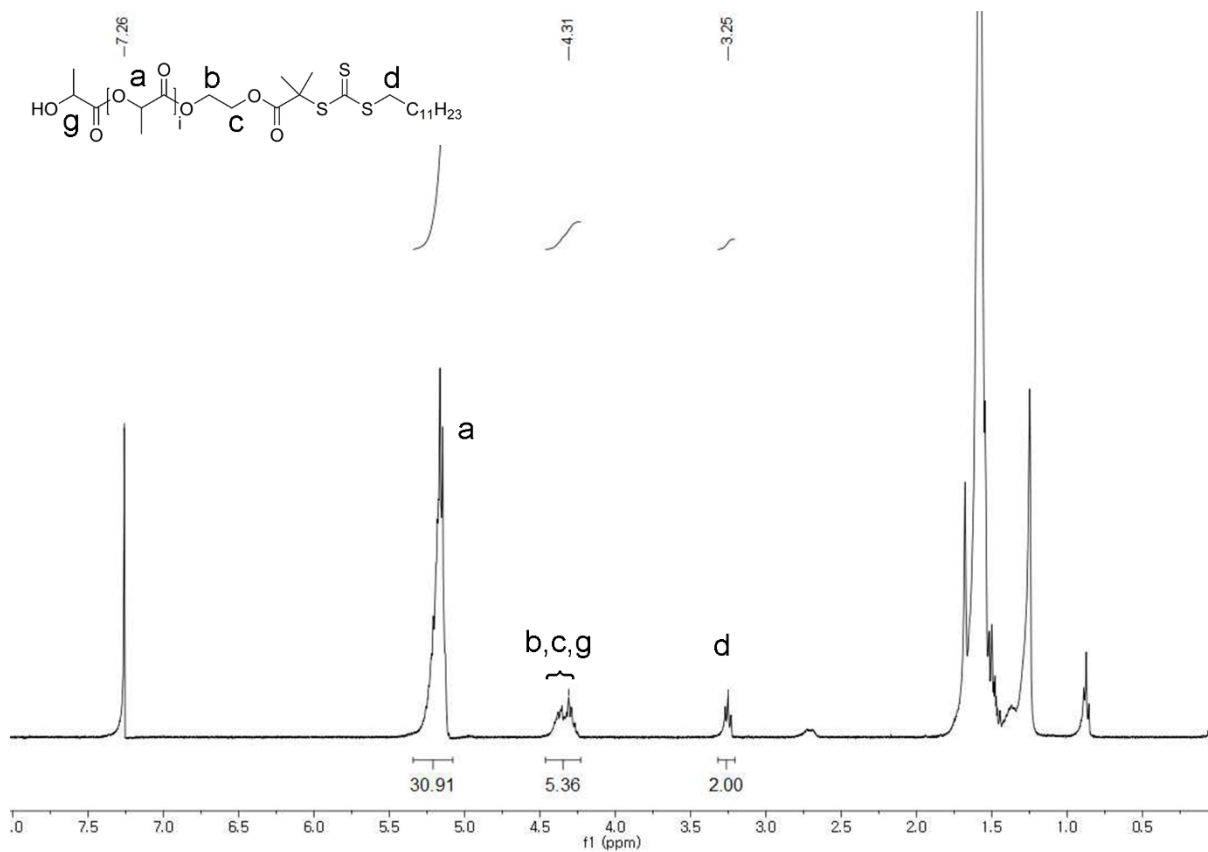


**Figure S12.** <sup>1</sup>H NMR spectrum of PLA<sub>31</sub> (400 MHz, CDCl<sub>3</sub>).

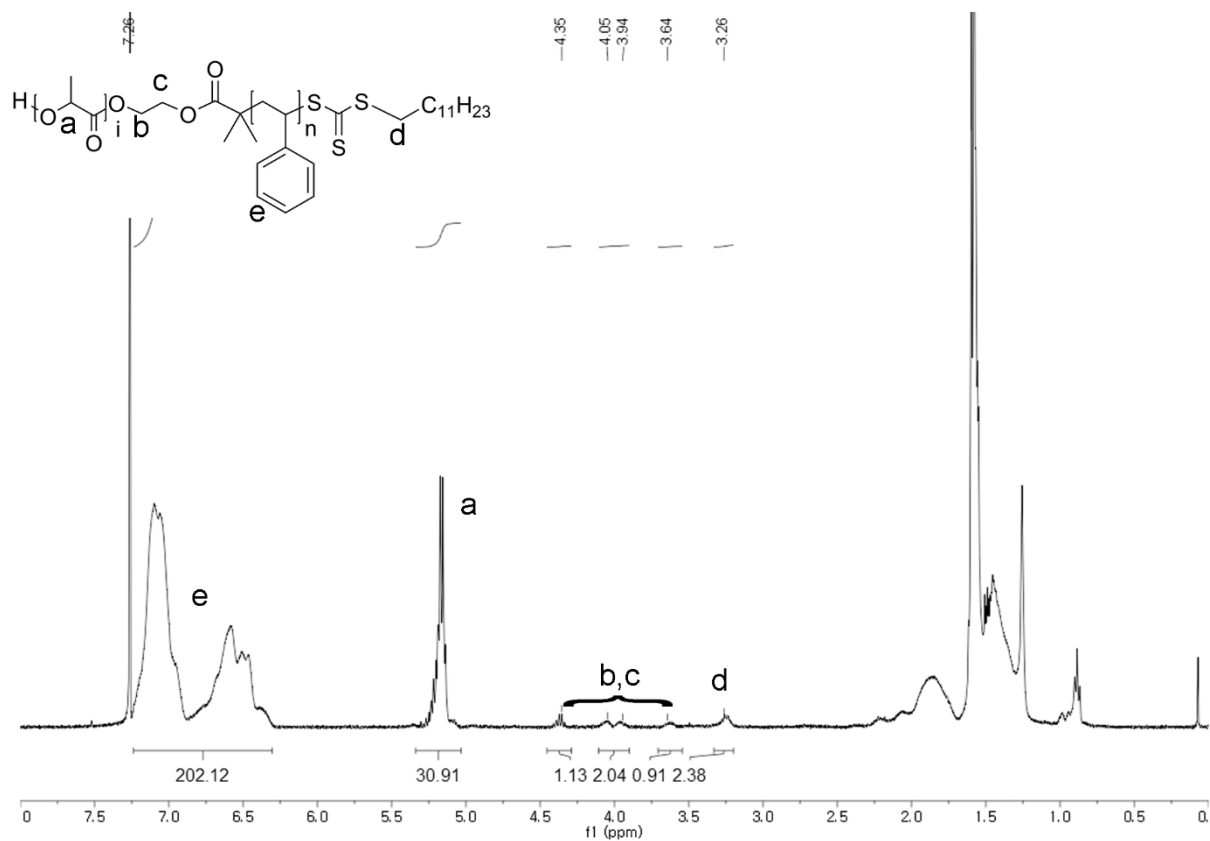


**Figure S13.** <sup>1</sup>H NMR spectrum of PLA<sub>31</sub>-b-PS<sub>40</sub> (400 MHz, CDCl<sub>3</sub>).

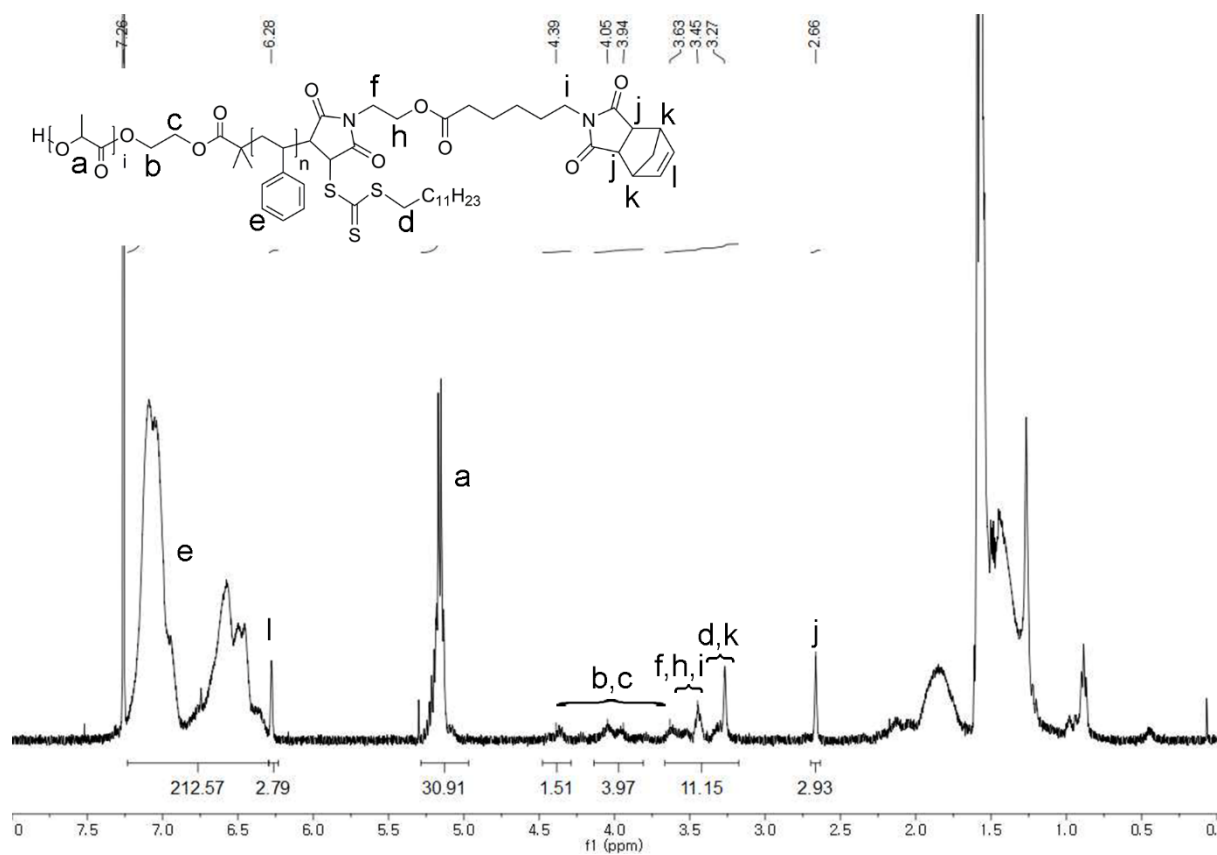


**Figure S14.** <sup>1</sup>H NMR spectrum of PLA<sub>31</sub>-b-PS<sub>40</sub>-branch (400 MHz, CDCl<sub>3</sub>).

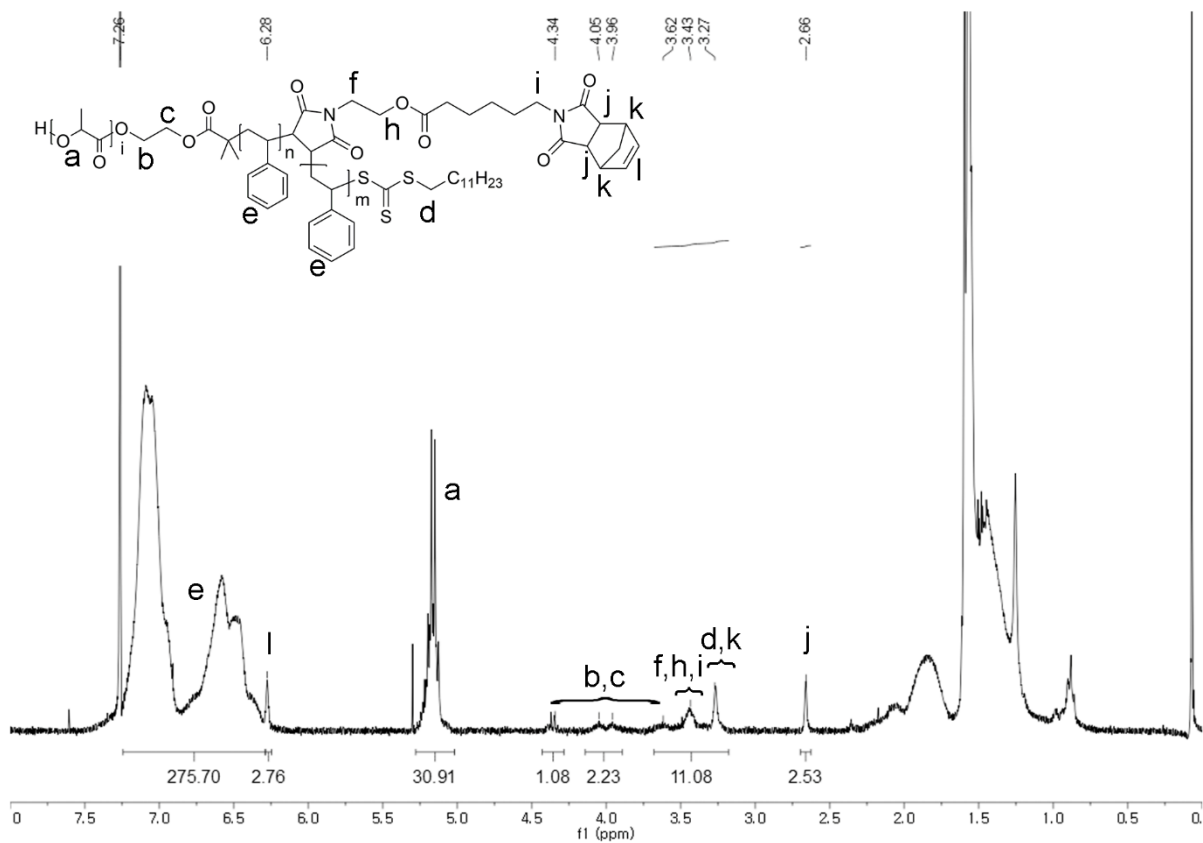


**Figure S15.** <sup>1</sup>H NMR spectrum of PLA<sub>31</sub>-b-PS<sub>40</sub>-branch-PS<sub>15</sub> (400 MHz, CDCl<sub>3</sub>).

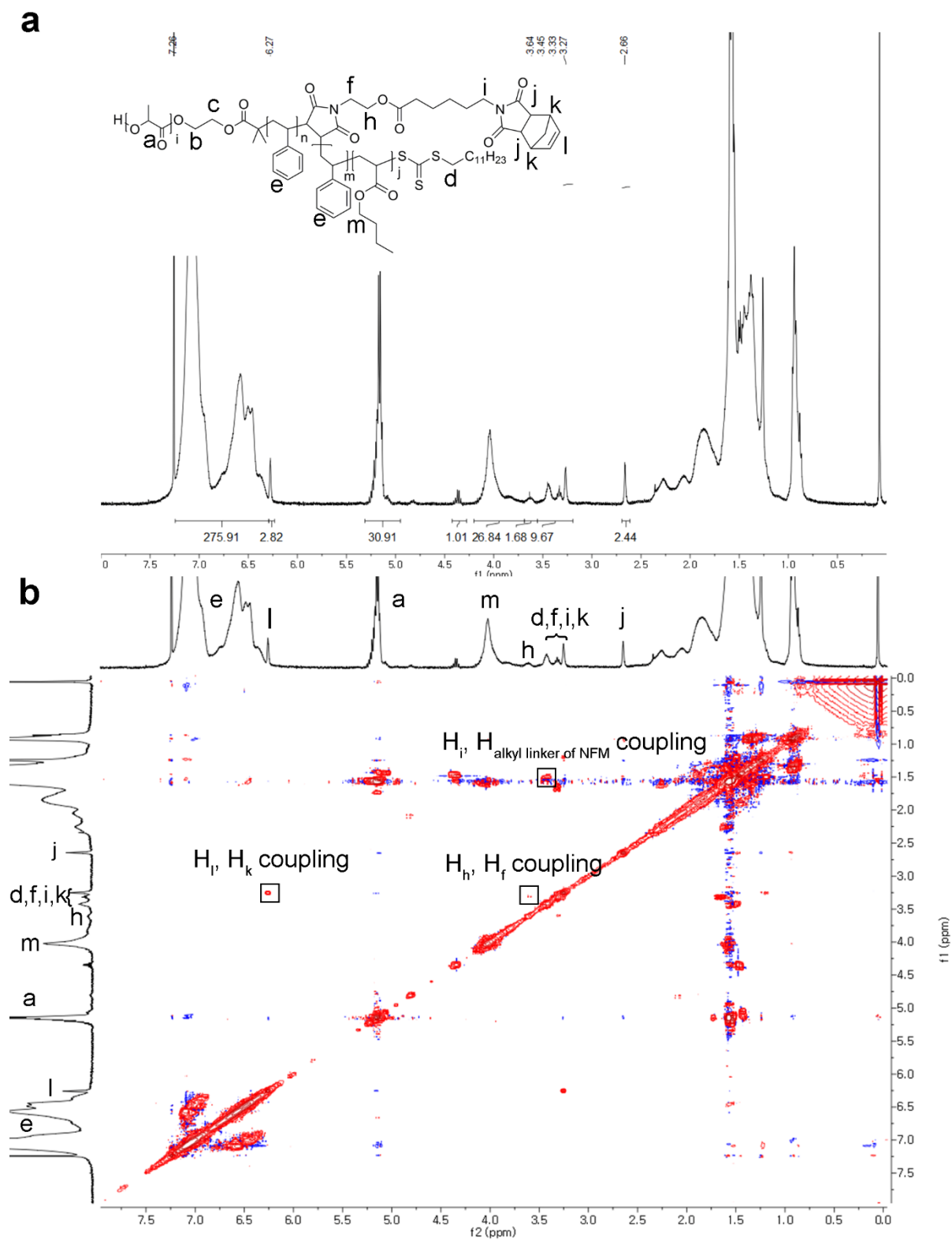


**Figure S16.** (a)  $^1\text{H}$  NMR and (b)  $^1\text{H}$ - $^1\text{H}$  COSY NMR spectrum of  $\text{PLA}_{31}\text{-}b\text{-PS}_{40}\text{-branch-PS}_{15}\text{-}b\text{-PnBA}_{13}$  (400 MHz,  $\text{CDCl}_3$ ).

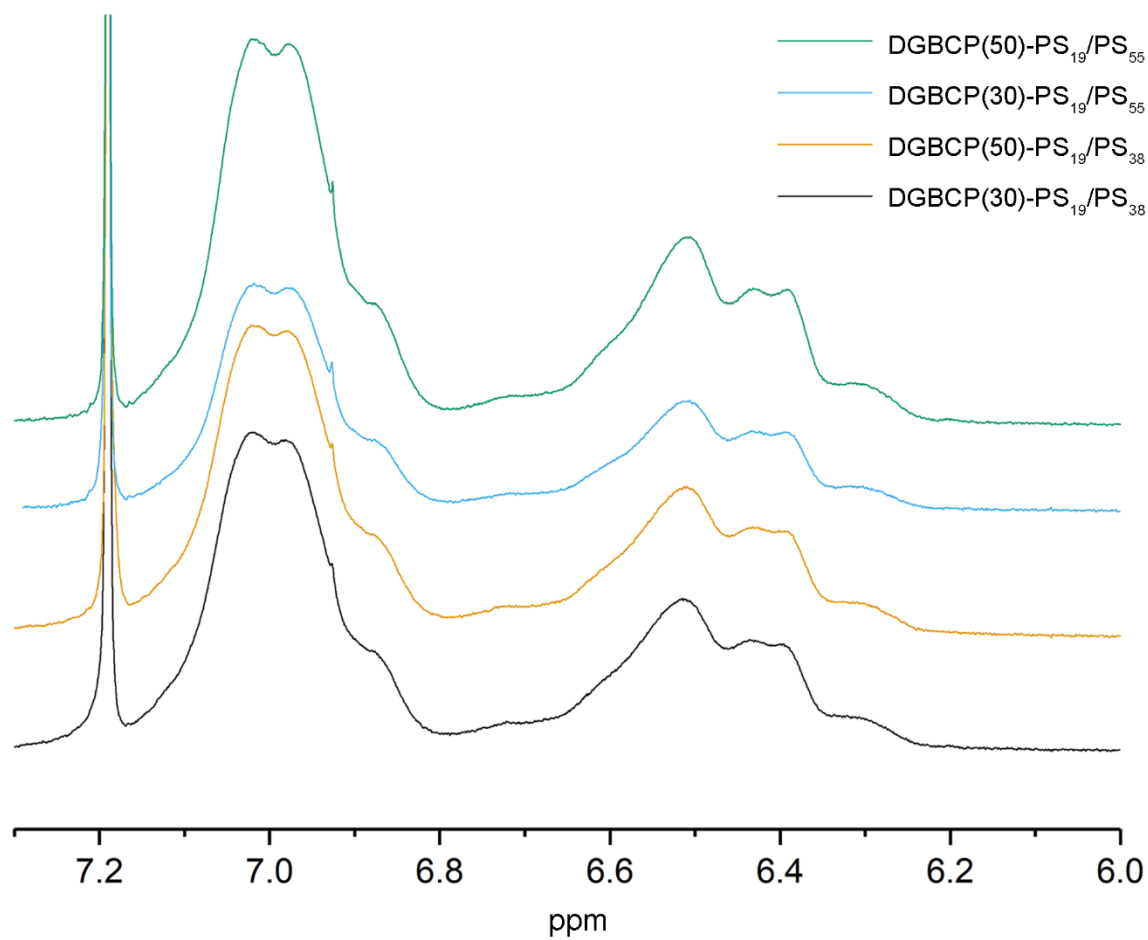


**Figure S17.** <sup>1</sup>H NMR spectra of DGBCPs-PS/PS indicating an absence of the olefinic proton signal at 6.28 ppm in the norbornenyl group (400 MHz, CDCl<sub>3</sub>).

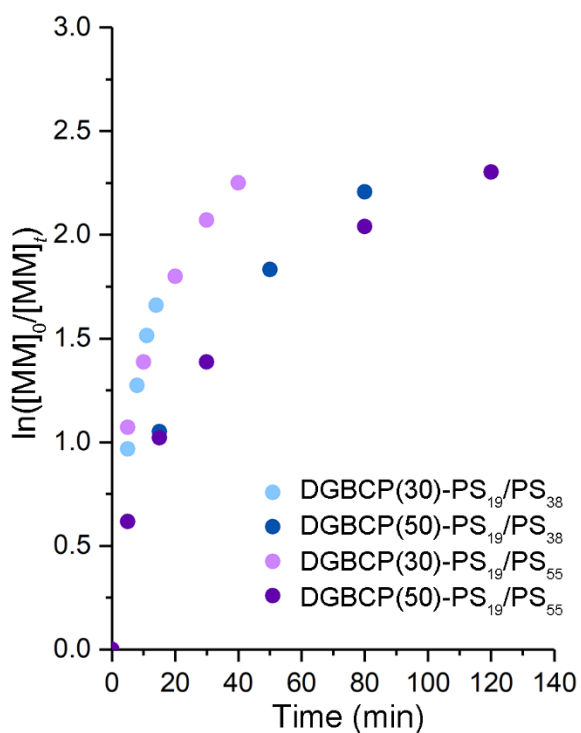


**Figure S18.** Dependence of  $\ln([MM]_0/[MM]_t)$  on time for ROMP of DGBCP-PS/PS. The reaction conditions are as follows:  $[MM]_0 = 0.03$  M for DGBCP(30)-PS<sub>19</sub>/PS<sub>38</sub>,  $[MM]_0 = 0.025$  M for DGBCP(50)-PS<sub>19</sub>/PS<sub>38</sub>,  $[MM]_0 = 0.015$  M for DGBCP(30)-PS<sub>19</sub>/PS<sub>55</sub>,  $[MM]_0 = 0.01$  M for DGBCP(50)-PS<sub>19</sub>/PS<sub>55</sub> in THF at room temperature.

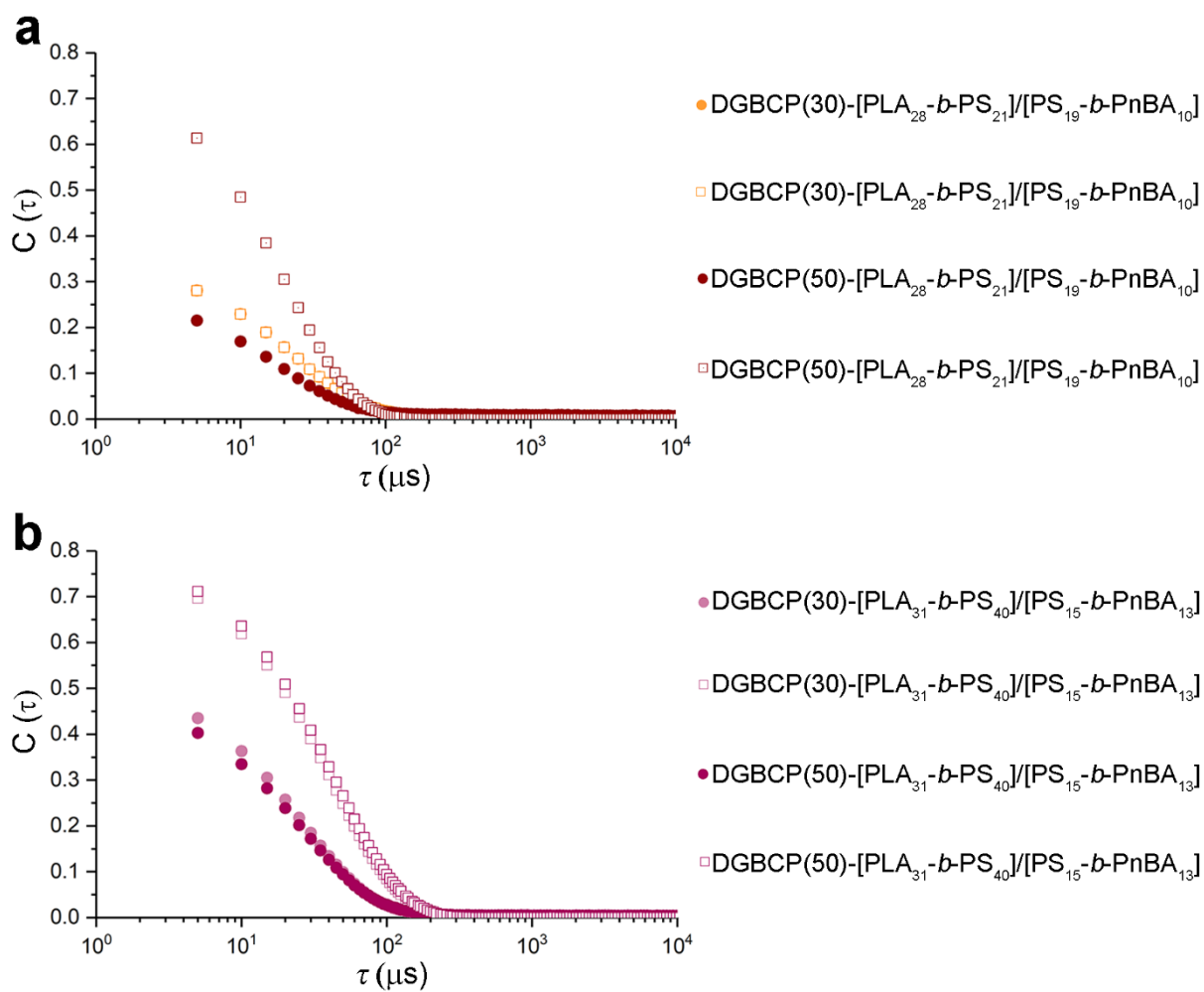


**Figure S19.** (a) Autocorrelation functions of DGBCP-[PLA<sub>28</sub>-*b*-PS<sub>21</sub>]/[PS<sub>19</sub>-*b*-PnBA<sub>10</sub>]. (b) Autocorrelation functions of DGBCP-[PLA<sub>31</sub>-*b*-PS<sub>40</sub>]/[PS<sub>15</sub>-*b*-PnBA<sub>13</sub>]. Filled circles and open squares represent the data of DGBCPs in DCM and MeCN, respectively.

**Dissipative Particle Dynamics (DPD) Simulation.** The simulation method presented in this study is based on dissipative particle dynamics (DPD) simulation originally proposed for the study of hydrodynamic behavior of complex fluids<sup>5,6</sup> and extended to polymeric systems.<sup>7,8</sup> In DPD simulation, each particle (bead) is regarded as a cluster of atoms or molecules and its dynamics is governed by Newton's equations of motion.

$$\frac{d\mathbf{r}_i}{dt} = \mathbf{v}_i \quad m_i \frac{d\mathbf{v}_i}{dt} = \mathbf{f}_i$$

where  $\mathbf{r}_i$ ,  $\mathbf{v}_i$ , and  $m_i$  are the position, velocity, and mass of  $i$ th particle, respectively. Mass of particle is typically set to 1 for the simplicity. The total force  $\mathbf{f}_i$  contains four parts for the polymeric system which contains an additional spring force as described below.

$$\mathbf{f}_i = \sum_{j \neq i} (\mathbf{F}_{ij}^C + \mathbf{F}_{ij}^D + \mathbf{F}_{ij}^R + \mathbf{F}_{ij}^S)$$

The conservative force  $\mathbf{F}_{ij}^C$  is a soft repulsion with the cutoff radius of 1 in this study.

$$\mathbf{F}_{ij}^C = \begin{cases} a_{ij}(1 - r_{ij})\hat{\mathbf{r}}_{ij} & r_{ij} < 1 \\ 0 & r_{ij} \geq 1 \end{cases}$$

where  $\mathbf{r}_{ij} = \mathbf{r}_i - \mathbf{r}_j$ ,  $r_{ij} = |\mathbf{r}_{ij}|$ ,  $\hat{\mathbf{r}}_{ij} = \mathbf{r}_{ij}/|\mathbf{r}_{ij}|$ , and  $a_{ij}$  is the maximum repulsion strength between  $i$ th and  $j$ th particles. The dissipative force  $\mathbf{F}_{ij}^D$  and the random force  $\mathbf{F}_{ij}^R$  act together as a thermostat to the DPD system.

$$\mathbf{F}_{ij}^D = -\gamma w^D(r_{ij})(\hat{\mathbf{r}}_{ij} \cdot \mathbf{v}_{ij})\hat{\mathbf{r}}_{ij}$$

$$\mathbf{F}_{ij}^R = \sigma w^R(r_{ij})\xi_{ij}\Delta t^{-1/2}\hat{\mathbf{r}}_{ij}$$

where  $\mathbf{v}_{ij} = \mathbf{v}_i - \mathbf{v}_j$ ,  $\gamma$  is dissipative parameter and  $\sigma$  is noise amplitude.  $w^D(r_{ij})$  and  $w^R(r_{ij})$  are weight functions for dissipative force and random force, respectively.  $\xi_{ij}$  is randomly fluctuating variable with Gaussian statistics and  $\Delta t$  is a simulation time step. In order to form a correct DPD thermostat, parameters and weight functions of these two forces

satisfy the relationship described below.

$$w^D(r_{ij}) = [w^R(r_{ij})]^2, \quad \sigma^2 = 2\gamma k_B T$$

where  $k_B$  is the Boltzmann constant and  $T$  is temperature. The distance dependent weight functions for dissipative and random forces are chosen to be the similar form with the conservative force for simplicity of the system.

$$w^D(r_{ij}) = [w^R(r_{ij})]^2 = \begin{cases} (1 - r_{ij})^2 & r_{ij} < 1 \\ 0 & r_{ij} \geq 1 \end{cases}$$

The spring force  $\mathbf{F}_{ij}^S$  to model the flexible polymer chain is described as  $\mathbf{F}_{ij}^S = -C\mathbf{r}_{ij}$  where  $C$  is a spring constant.

In this study, Newton's equations of motions are integrated using modified version of Velocity-Verlet integrator developed by Groot and Warren.<sup>6,7</sup> In this algorithm, equations of motions are integrated from time  $t$  to  $t + \Delta t$  by two-step process: First, an intermediate velocity  $\tilde{\mathbf{v}}_i(t + \Delta t)$  is pre-determined before the forces are updated.

$$\mathbf{r}_i(t + \Delta t) = \mathbf{r}_i(t)\Delta t + \mathbf{v}_i(t)\Delta t^2 + \frac{1}{2}\mathbf{f}_i(t)\Delta t^2$$

$$\tilde{\mathbf{v}}_i(t + \Delta t) = \tilde{\mathbf{v}}_i(t) + \lambda\mathbf{f}_i(t)\Delta t$$

Then, forces and velocities at  $t + \Delta t$  are updated using intermediate velocity.

$$\mathbf{f}_i(t + \Delta t) = \mathbf{f}_i(\mathbf{r}_i(t + \Delta t), \tilde{\mathbf{v}}_i(t + \Delta t))$$

$$\mathbf{v}_i(t + \Delta t) = \mathbf{v}_i(t) + \frac{1}{2}(\mathbf{f}_i(t), \mathbf{f}_i(t + \Delta t))\Delta t$$

$\lambda$  in an intermediate velocity equation is tuning parameter for the higher-order correction of integration. From the previous studies, stable temperature control is realized when  $\lambda = 0.65$  with a very large time-step  $\Delta t$ . In this study, we set  $\sigma = 3.0$ ,  $C = 4.0$ ,  $\lambda = 0.65$ , and  $\Delta t = 0.05$  for all simulation conditions.

In this study, we simulated three types of DGBCPs as shown in Figure S20. Green

bead (denoted by A) represents PLA block, blue bead (denoted by B) represents PS block, and orange bead (denoted by C) represents PnBA block. Our modeled DGBCPs contains  $A_2B_3C$  BMMMs are linearly connected at certain branch site of B monomer (denoted by  $B^*$ ). In this model, three branch sites are possible, so we can construct three types of linearly connected  $m$   $A_2B_3C$  triblock copolymers models as shown in Figure S20:  $(A_2BB^*BC)_m$ ,  $(A_2B^*BBC)_m$ , and  $(A_2BBB^*C)_m$ .

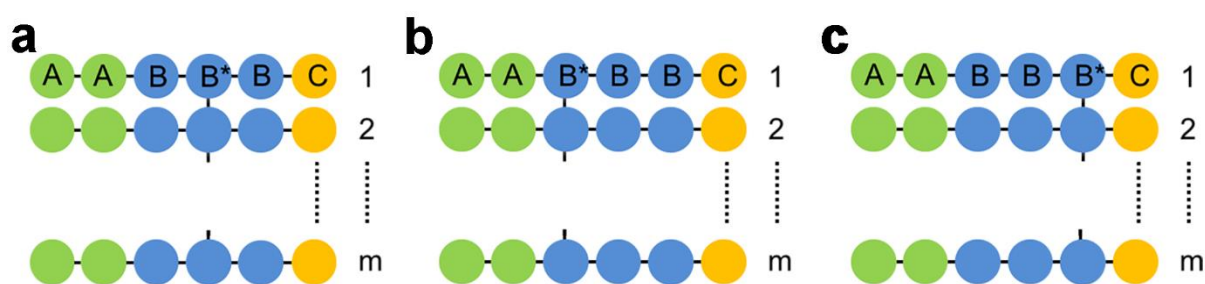


**Figure S20.** Simulated DGBCP models with different branch sites and length: (a)  $(A_2BB^*BC)_m$ . (b)  $(A_2B^*BBC)_m$ . (c)  $(A_2BBB^*C)_m$ .

We also simulated solvent beads (denoted by S) explicitly to study the self-assembly behavior of DGBCPs in solution. The size of simulation box is  $40 \times 40 \times 40$  with a particle number density of 3.0. As a result, the total number of DPD particles in the simulation box is 192000. The total number of DGBCP (A, B, and C) beads and solvent (S) beads are 9600 and 182400, respectively, so that the volume density of DGBCPs in solution is set to 5%.

Pairwise repulsion strength  $a_{ij}$  is determined as follow. We set  $a_{AB} = a_{BC} = 50.0$  and  $a_{AC} = 100.0$  based on the high incompatibility between PLA, PS, and PnBA. We set  $a_{AS} = 25.0$ ,  $a_{BS} = 200.0$ , and  $a_{CS} = 27.0$  according to relative solubility of each block to MeCN. Pairwise repulsion strength between the same type of beads  $a_{ii}$  ( $i=A, B, C$ , and S) is

set to 25.0. All simulation in this study are conducted from complete random initial configuration of DPD particles for  $10^6$  DPD time steps which is enough for the equilibrium of the system.

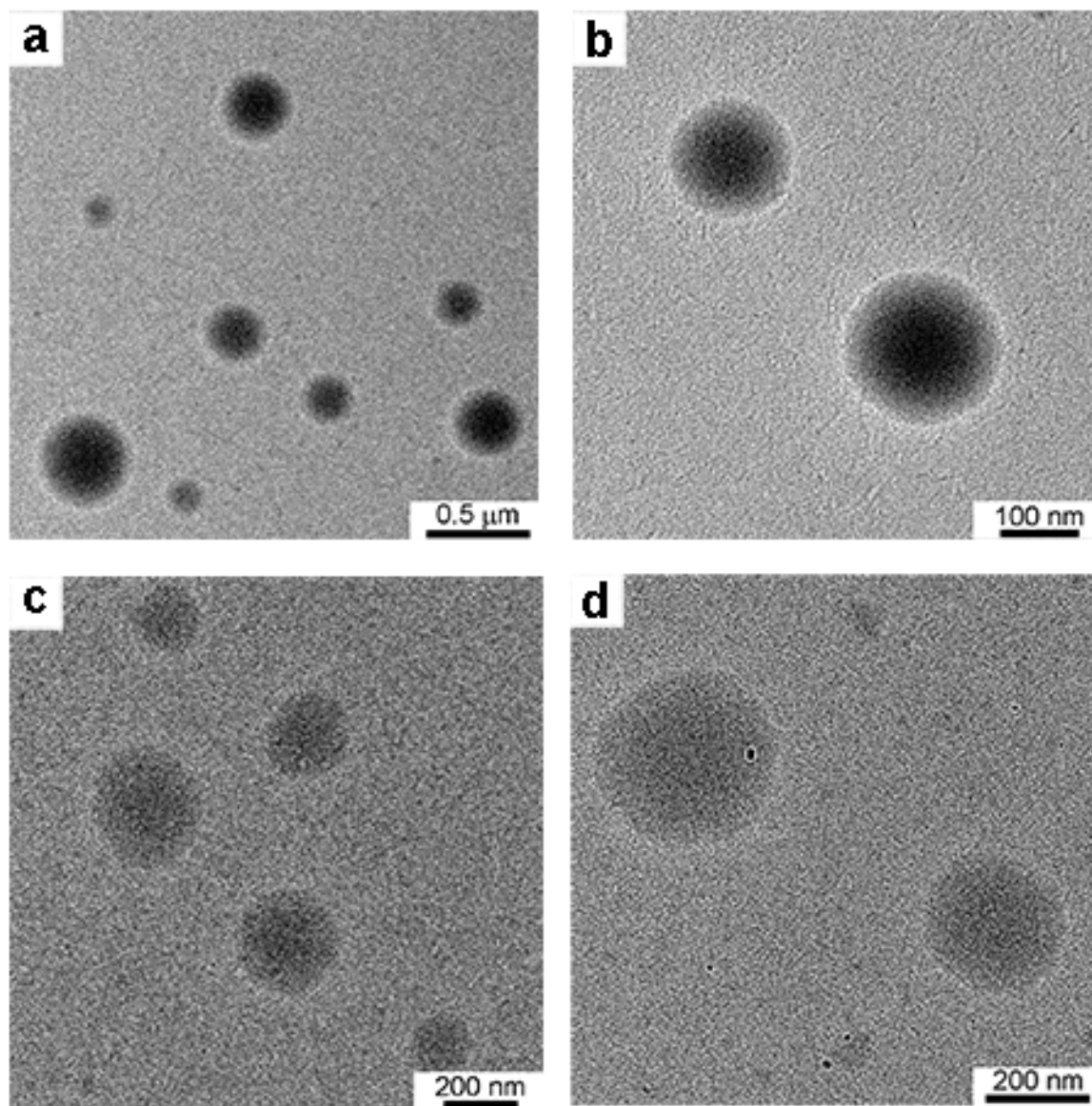


**Figure S21.** TEM images of  $\text{PLA}_{28}\text{-}b\text{-PS}_{21}\text{-branch-PS}_{19}\text{-}b\text{-PnBA}_{10}$  BMMM, at low (a) and high (b) magnification. TEM images of  $\text{PLA}_{31}\text{-}b\text{-PS}_{40}\text{-branch-PS}_{15}\text{-}b\text{-PnBA}_{13}$  BMMM, at low (c) and high (d) magnification.

## References

- <sup>1</sup> Bates, C. M.; Chang, A. B.; Momčilović, N.; Jones, S. C.; Grubbs, R. H. ABA Triblock Brush Polymers: Synthesis, Self-Assembly, Conductivity, and Rheological Properties. *Macromolecules* **2015**, *48*, 4967–4973.
- <sup>2</sup> Zhao, J.; Xu, R.; Luo, G.; Wu, J.; Xia, H. Self-healing poly(siloxane-urethane) elastomers with remoldability, shape memory and biocompatibility. *Polym. Chem.* **2016**, *7*, 7278–7286.
- <sup>3</sup> Lai, J. T.; Filla, D.; Shea, R. Functional Polymers from Novel Carboxyl-Terminated Trithiocarbonates as Highly Efficient RAFT Agents. *Macromolecules* **2002**, *35*, 6754–6756.
- <sup>4</sup> Oh, J.; Seo, M. Photoinitiated Polymerization-Induced Microphase Separation for the Preparation of Nanoporous Polymer Films. *ACS Macro Lett.* **2015**, *4*, 1244–1248.
- <sup>5</sup> Hoogerbrugge, P. J.; Koelman, J. M. V. A. Simulating Microscopic Hydrodynamic Phenomena with Dissipative Particle Dynamics. *Europhys. Lett.* **1992**, *19*, 155–160.
- <sup>6</sup> Koelman, J. M. V. A.; Hoogerbrugge, P. J. Dynamic Simulations of Hard-Sphere Suspensions Under Steady Shear. *Europhys. Lett.* **1993**, *21*, 363–368.
- <sup>7</sup> Groot, R. D.; Warren, P. B. Dissipative Particle Dynamics: Bridging the Gap between Atomistic and Mesoscopic Simulation. *J. Chem. Phys.* **1997**, *107*, 4423–4435.
- <sup>8</sup> Groot, R. D.; Madden, T. J. Dynamic Simulation of Diblock Copolymer Microphase Separation. *J. Chem. Phys.* **1998**, *108*, 8713–8724.